Terahertz dual-beam leaky-wave antenna based on composite spoof surface plasmon waveguide*

BAI Yukun and LI Sen**
Tianjin Key Laboratory of Film Electronic and Communication Devices, Engineering Research Center of Optoelectronic Devices and Communication Technology, Ministry of Education, School of Integrated Circuit Science and Engineering, Tianjin University of Technology, Tianjin 300384, China

(Received 30 June 2022; Revised 10 August 2022)

In this paper, we propose a single-port dual-beam leaky-wave antenna (LWA) in the terahertz (THz) band based on a composite spoof surface plasmon polariton (SSPP) waveguide. The antenna can generate three independent transmission channels by exciting two independent modes inherent to hole and groove structures, respectively. By periodic modulation of the hole and groove structures, we achieve dual-beam scanning through a broad radiation angle using only the −1st space harmonics of the two modes, hence avoiding the instability of the −2rd space harmonic. Within the operating frequency range of 0.62—0.85 THz, the gain ranges from 13.5 dBi to 17 dBi for the backward beam, and from 6 dBi to 11.8 dBi for the forward beam. The antenna can accomplish continuous backward beam through broadside to forward beam scanning with a total scanning range of 116° and an average efficiency of about 92%. The antenna exhibits a great potential in the design of multi-transceiver radar system in the THz band and multi-beam LWAs.
Document code: A **Article ID:** 1673-1905(2023)02-0072-5
DOI https://doi.org/10.1007/s11801-023-2118-x

In recent years, with the continuous development of terahertz (THz) communication technology, leaky-wave antennas (LWAs) have received extensive attention in the field of THz wireless systems due to their small size, frequency beam steering capability[1-3], and ease of manufacture. According to the modulations imposed on the waveguide, LWA can be roughly divided into three categories, namely uniform, quasi-periodic and periodic ones. The LWA in this paper is based on a periodically modulated surface wave waveguide, namely, the surface plasmon (SP) waveguide, which is an electromagnetic phenomenon caused by the collective oscillation of free electrons at the metal-substrate interface. Conventionally operating in the optical regime, the surface wave propagates along the interface and decays exponentially in the direction perpendicular to the interface. In 2004, PENDRY et al[4] theoretically showed that metal surfaces with defective structures (such as grooves, holes, etc.) can support surface plasmons, namely spoof surface plasmon polaritons (SSPPs), in the microwave and THz frequency bands. SSPPs allow for high field confinement which can effectively eliminate channel cross-talks. Furthermore, the modal dispersion characteristics of SSPPs can be tailored efficiently by means of the geomentrical shapes, dimensions and material properties of the SSPP unit structure[5-7]. Due to the aforementioned merits of SSPPs, researchers have successively proposed various SSPP waveguide structures which were used widely in microwave and THz circuits and devices[8-21].

With the development and research of wireless communication technology, dual-beam and multi-beam LWAs have received much attention, and have shown attractive promises in mobile vehicle radar, medical sensors, aviation navigation tracking technology, etc. The multi-beam antenna can radiate multiple beams in space, and realize simultaneous interaction with multiple targets and coverage of multiple areas at the same time. In the multiple-input multiple-output (MIMO) system, the multi-beam antenna can reduce the number of transceiver antennas, simplify the system complexity, and increase the system capacity. In Refs.[15] and [16], a dual-beam LWA using one-dimensional three-period microstrip structure was constructed based on the −1st and −2rd two space harmonic modes. Usually, −2rd space harmonic is not as stable as −1st space harmonic. In Ref.[17], the substrate integrated waveguide-based LWA array radiates two beams symmetrically. The LWA array can achieve a wider impedance bandwidth and an increased scanning range including broadside. In Ref.[18], dual-beam radiation is generated by corrugating two grooves with different periods based on two −1st space harmonics, exhibiting discontinuous scanning range and limited gains.

* This work has been supported by the Natural Science Foundation of Tianjin (No.19JCYBJC16100), and the Tianjin Innovation and Entrepreneurship Training Program (No.202210060027).
** E-mail: sen17602607235@163.com

In this paper, we propose a single-port dual-beam LWA based on a composite waveguide structure in the THz band. The antenna adopts a single-port feed to effectively reduce the overall size. With an instantaneous wide scanning range through broadside enabled by a simple feeding structure and dual beams, it exhibits stable and satisfactory performance in the THz regime.

Corrugated U-shaped grooves at the upper and lower edges of the SSPP waveguide have the same period and are symmetrical with respect to the midline of the guiding stripe. Rectangular holes are corrugated along the strip midline. Two beams are generated by the periodic modulations of the edge grooves and middle rectangular holes, respectively. The overall schematic diagram of the antenna is shown in Fig.1, with an overall size of $L\times W$=9 569.9 μm×975 μm. The unit structure is encircled by the red square. The double-layer structure consists of a dielectric substrate with a thickness of 7.5 μm, made of F4B with dielectric constant ε_r=2.65 and loss tangent tanδ=0.001, and the designed metal thin film on top with a thickness of 0.27 μm.

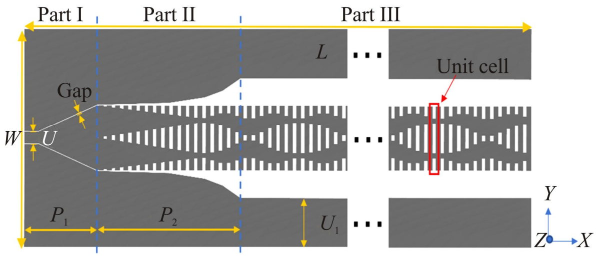

Fig.1 Schematic diagram of overall structure of the proposed antenna

The antenna is mainly divided into three parts, as shown in Fig.1. The first part is the feeding part of the antenna, which uses the coplanar waveguide (CPW) with dimensions U=52.5 μm, Gap=2.7 μm, P_1=392.6 μm as the input port with a 50 Ω characteristic impedance. The second part is the transition part with a length of P_2=749.3 μm. The gradient structure is used to achieve the momentum matching, in which the rectangular hole depth changes from of 2.14 μm to 130.91 μm and the upper and lower groove depth changes from the minimum of 0.87 μm to the maximum of 53.55 μm, so that the TEM wave is converted into the TM wave smoothly. The third part is the transmission line part, which consists of three independent channels. The upper and lower channels are U-shaped groove structures, which are symmetrical with respect to the longitudinal midline. The middle channel is a rectangular hole structure along the midline. Two metal strips with a width of U_1=225 μm are loaded on both sides of the SSPP waveguide to make the radiation on the E plane more concentrated.

The SSPP unit structure is composed of two U-shaped grooves on the upper and lower edges, and a rectangular hole in the middle, as shown in Fig.2(a). Blue represents the dielectric substrate, and gray is the metal sheet. The geometric parameters are as follows, W_1=12.75 μm, W_2=16.95 μm, L_1=285 μm, L_2=54 μm, L_3=132 μm. By using the eigenmode solver in the CST microwave studio on the unit structure, the electrical fields E_x of two composite modes are obtained, as shown in Fig.2(b) and (c). The dispersion curves of the two modes are also obtained as shown in Fig.2(d). It can be seen that the dispersion curves of mode 1 (determined by the rectangular hole) are not sensitive to the change of L_2, whereas those of mode 2 (determined by the U-shaped groove) are not sensitive to the change of L_3. The cutoff frequencies of both sets decrease with the increase of depths L_2 and L_3.

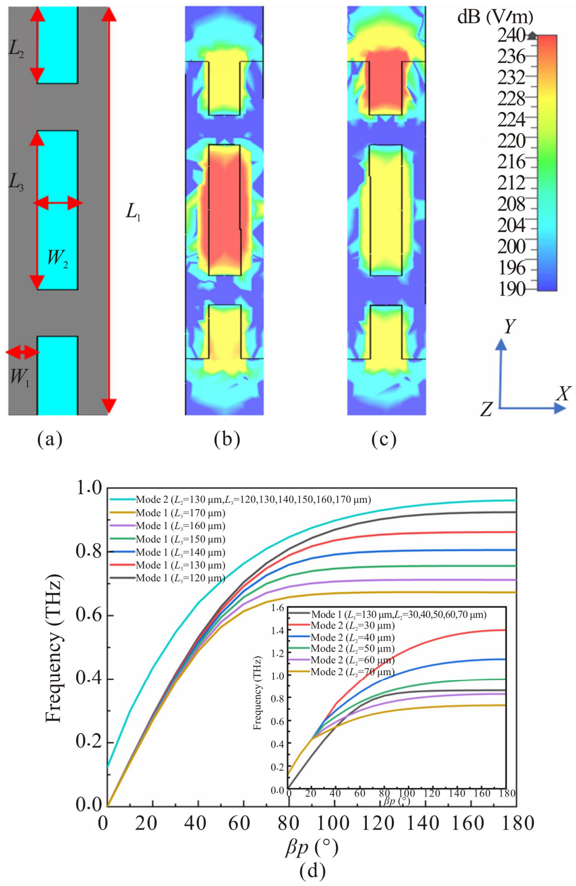

Fig.2 (a) Schematic diagram of SSPP unit structure; (b) Surface current distribution of mode 1; (c) Surface current distribution of mode 2; (d) Dispersion diagram of SSPP unit with varying L_2 and L_3, respectively

According to the theory of SMRS, the SSPP surface wave can be radiated into the space by imposing the sinusoidal modulation on the SSPP waveguide along the propagation direction. Infinite space harmonics can be excited, but we use only the −1st space harmonic. The radiation angle with respect to the z axis can be calculated as

$$\theta_{-1}=\arcsin\left(\sqrt{1+X'^2}-\frac{2\pi}{k_0 p}\right), \tag{1}$$

where X' is the normalized average surface reactance, k_0

is the free-space wavenumber, and p is the modulation period.

With the surface-wave propagation along the x axis, the surface impedance can be calculated as follows

$$Z_{\mathrm{surf}} = \mathrm{j}X_{\mathrm{s}}\left[1+M\cos\left(\frac{2\pi x}{p}\right)\right], \tag{2}$$

where $X_{\mathrm{s}}=\eta_0 X'$, X_{s} is average surface reactance, η_0 is the wave impedance in free space, and M is the modulation factor.

From the Floquet's theorem, the propagation constant β_n of the nth space harmonic is

$$\beta_n p=\beta_0 p+2n\pi, n=0,\pm1,\pm2,\ldots, \tag{3}$$

where β_0 is that of the 0th space harmonic. Furthermore, the relationship between the surface impedance and the propagation constant β_x along the x axis, which provides a practical means to implement the required surface impedance, can be expressed as

$$Z_{\mathrm{surf}}(x)=\eta_0\sqrt{1-\left(\beta_x/\beta_0\right)^2}. \tag{4}$$

We design a dual-beam LWA based on the sinusoidally modulated SSPPs with a radiation angle of −35° for the backward beam and +20° for the forward beam at the frequency of 0.7 THz. Take the backward beam as an example. Given the radiation angle and the modulation period m_1=254.7 μm, the value of X' is obtained from Eq.(1) to be 1.13. Substituting X'=1.13 and M=0.65 into Eq.(2), the values of Z_{surf} can be solved. The surface impedance Z_{surf} ranges from 149.11 Ω to 702.96 Ω. Finally, the surface impedance Z_{surf} is sampled at equidistance within a period according to Eq.(2) and the groove depths of each sample unit are determined through Eq.(4) and the dispersion curves. Similar procedure can be carried out for the formation of the forward beam induced by the rectangular slots. Thus, the LWA satisfying the specifications can be constructed.

The schematic diagram of the designed structure in a single composite modulation period is shown in Fig.3(a). The period of the upper and lower U-shaped grooves is m_1=254.7 μm, and the depth of each groove within a period is h_1=54 μm, h_2=43.5 μm, and h_3=33 μm, respectively. The period of the middle rectangular hole is m_2=509.4 μm, and the depth of each slot within a period is h_4=132 μm, h_5=126 μm, h_6=112.5 μm, h_7=87 μm, h_8=51 μm, and h_9=24 μm. Fig.3(b) and (c) are the single-period dispersion diagrams for periods m_1 and m_2, respectively. The black line represents the light line. It can be seen from the figures that these two modulated structures can effectively excite two −1st spatial harmonics in the frequency band from 0.62 THz to 0.85 THz, respectively, which leads to a dual-beam LWA.

The S-parameter of the antenna is shown in Fig.4. In the frequency band from 0.62 THz to 0.85 THz, S_{11} is lower than −10 dB, indicating that satisfactory impedance matching is achieved.

In the space above the antenna, the scanning angle of the backward beam in the frequency band from 0.62 THz to 0.85 THz is from −36° to +24°, and that of the forward beam is from +22° to +80°. Fig.5 shows the simulated radiation patterns in the E-plane.

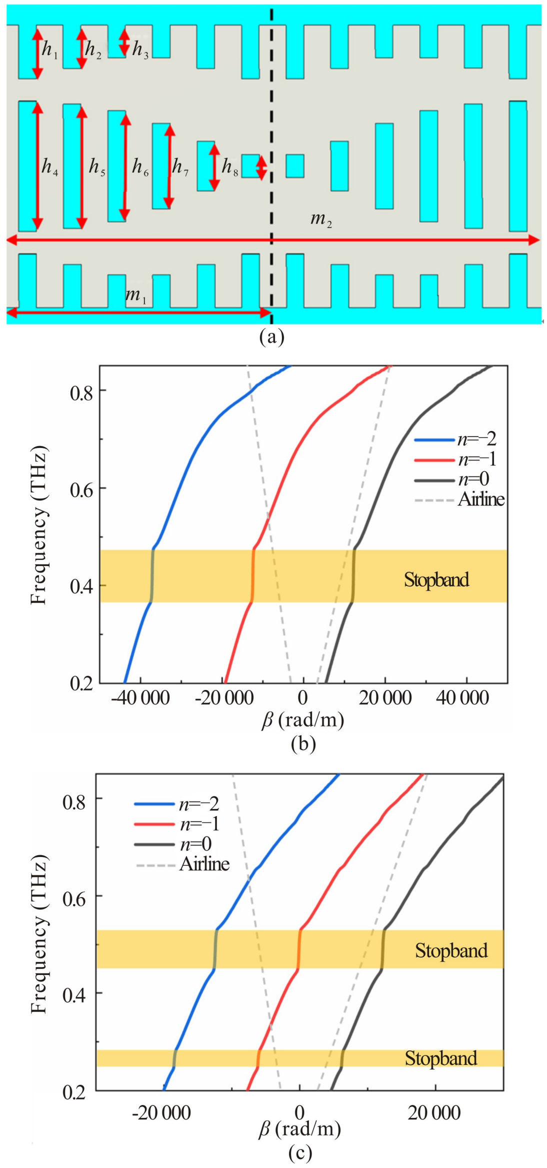

Fig.3 (a) Schematic diagram of an SSPP structure in a single composite modulation period; (b) Dispersion diagram with period m_1; (c) Dispersion diagram with period m_2

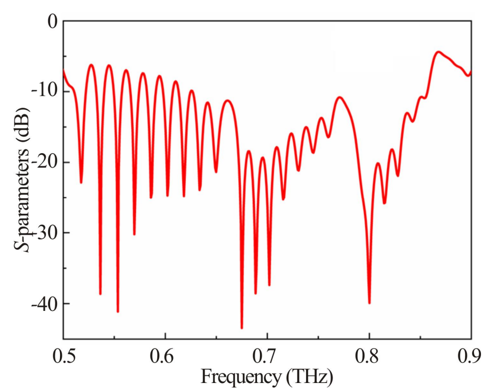

Fig.4 Simulation results of S-parameters

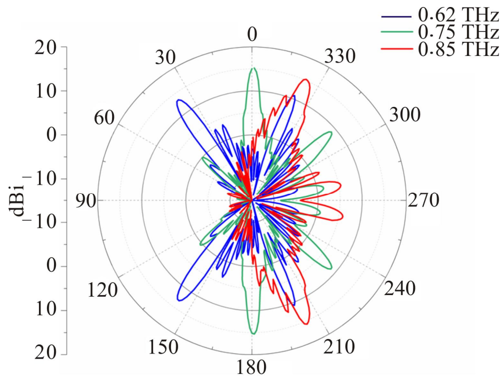

Fig.5 Simulated radiation patterns in E-plane at 0.62 THz, 0.75 THz, and 0.85 THz

The antenna designed in this article shows good performance in the THz regime compared with previously published dual-beam LWAs counterparts, as indicated in Tab.1. The antenna can achieve a continuous beam scanning from backward through broadside to forward. It can be seen from Fig.6 that the maximum scanning angle of the backward beam is greater than the initial scanning angle of the forward beam, namely, the radiation coverage of the two beams overlaps with each other. In other words, the dual-beam antenna has a large continuous total scanning range of 116°. Fig.7 shows the radiation

Tab.1 Comparison between the LWA proposed in this paper and the previously published literatures

Ref.	Frequency	Through broadside	Scanning range (°)	Gain (dBi)
[15]	5.6—6.0 GHz	No	36—42 −46—−34	2.8—0.9 −4.8—−1.3
[16]	57—63 GHz	No	22— 28 −31— −20	20—25 21—23
[17]	5.2—7.5 GHz	Yes	−16—60 −62—14	4.5—13 5.5—13
[18]	9—12 GHz	No	13—42.5 −68—−11	9—9.1 5.8—8
This work	0.62—0.85 THz	Yes	22—80 −36—24	6—11.8 13.5—17

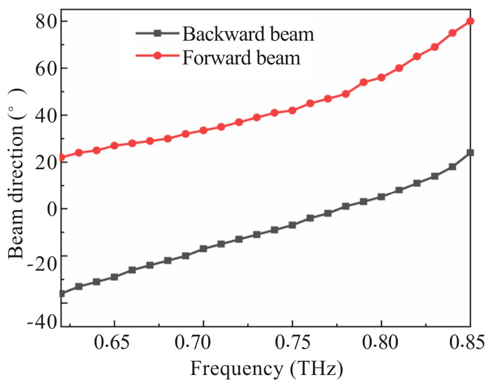

Fig.6 Simulated radiation directions of the forward and backward beams from 0.62 THz to 0.85 THz

efficiency of the antenna. The average gain of the antenna in the operating band can reach 92%. Fig.8 is a diagram of the antenna gain, in which the gain of the backward beam is from 13.5 dBi to 17 dBi, and that of the forward beam from 6 dBi to 11.8 dBi, which indicates a comparatively high gain.

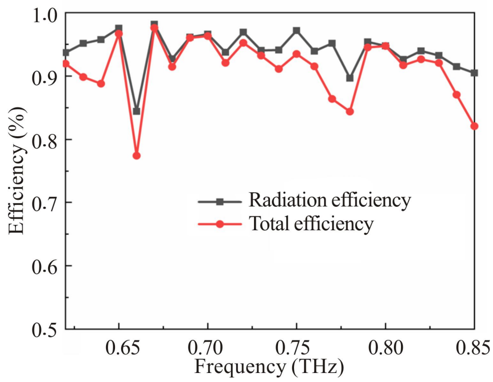

Fig.7 Antenna radiation efficiency from 0.62 THz to 0.85 THz

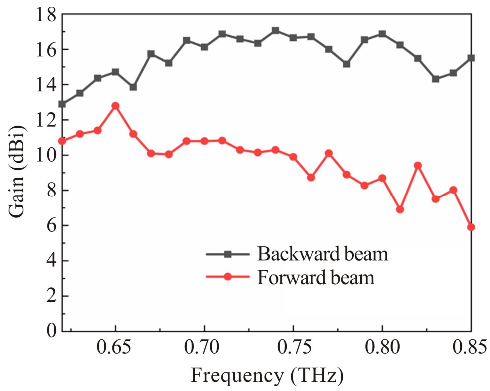

Fig.8 Simulated gain of the forward and backward beams

In this paper, a three-channel dual-beam LWA based on a composite SSPP unit structure is proposed to operate in the THz regime. We can further conclude that the concept-proved LWA can achieve multi-channel excitation of multi-beam radiation to meet the demands of different scenarios.

Statements and Declarations

The authors declare that there are no conflicts of interest related to this article.

References

[1] KARL N J, MCKINNEY R W, MONNAI Y, et al. Frequency-division multiplexing in the terahertz range using a leaky-wave antenna[J]. Nature photonics, 2015, 9：717-720.

[2] LU P, HADDAD T, SIEVERT B, et al. InP-based THz beam-steering leaky-wave antenna[J]. IEEE transactions on terahertz science and technology, 2020, 11(2)：218-230.

[3] JACKSON D R, CALOZ C, ITOH T. Leaky-wave antennas[J]. IEEE, 2012, 100(7)：2194-2206.

[4] PENDRY J B, MARTÍN-MORENO L, GARCIA-VIDAL F J. Mimicking surface plasmons with structured sufaces[J]. Science, 2004, 305(5685)：847-848.

[5] SUTINJO A, OKONIEWSKI M, JOHNSTON R H. Radiation from fast and slow traveling waves[J]. IEEE antennas and propagation magazine, 2008, 50(4)：175-181.

[6] SHEN X P. Conformal surface plasmons propagating on ultrathin and flexible films[J]. Proceedings of the national academy of sciences, 2013, 110(1)：40-45.

[7] YANG T. Open waveguide based on low frequency spoof surface plasmon polaritons[J]. Journal of electromagnetic analysis and applications, 2013, 5(2)：58-62.

[8] ZHANG Q L, CHEN B J, CHAN K F, et al. High-gain millimeter-wave antennas based on spoof surface plasmon polaritons[J]. IEEE transactions on antennas and propagation, 2020, 68(6)：4320-4331.

[9] CHAI B, LI Y J, BAI Y K. A wide-band continuous-beam-scanning leaky-wave antenna with a stable gain fed by spoof surface plasmon polaritons[J]. Optoelectronics letters, 2022, (4)：210-214.

[10] ZHANG Q L, CHEN B J, CHAN K F, et al. Terahertz circularly and linearly polarized leaky-wave antennas based on spin-orbit interaction of spoof surface plasmon polaritons[J]. IEEE transactions on antennas and propagation, 2021, 69 (8)：4347-4358.

[11] KONG G S, MA H F, CAI B G, et al. Continuous leaky-wave scanning using periodically modulated spoof plasmonic waveguide[J]. Scientific reports, 2016, 6：29600.

[12] LIAO D, ZHANG Y, WANG H. Wide-angle frequency-controlled beam-scanning antenna fed by standing wave based on the cutoff characteristics of spoof surface plasmon polaritons[J]. IEEE antennas and wireless propagation letters, 2018, 17(7)：1238-1241.

[13] GUAN D F, PENG Y, ZHANG Q, et al. Hybrid spoof surface plasmon polariton and substrate integrated waveguide transmission line and its application in filter[J]. IEEE transactions on microwave theory & techniques, 2017, 65(12)：4925-4932.

[14] YE L, WEI Z, OFORI-OKAI B K, et al. Super subwavelength guiding and rejecting of terahertz spoof SPPs enabled by planar plasmonic waveguides and notch filters based on spiral-shaped units[J]. Journal of lightwave technology, 2018, 36(20)：4988-4994.

[15] MA Z L, JIANG L J. One-dimensional triple periodic dual-beam microstrip leaky-wave antenna[J]. IEEE antennas and wireless propagation letters, 2015, 14：390-393.

[16] MA Z L, NG K B, CHAN C H, et al. A novel supercell based dielectric grating dual-beam leaky-wave antenna for 60-GHz applications[J]. IEEE transactions on antennas & propagation, 2016, 64(12)：5521-5526.

[17] GENG Y, WANG J, LI Z, et al. A compact circularly polarized half-mode substrate integrated waveguide-based leaky-wave antenna array with wide range of dual-beam scanning[J]. International journal of RF and microwave computer-aided engineering, 2022, 32(4)：e23074.

[18] ZHANG C, REN J, DU X, et al. Dual-beam leaky-wave antenna based on dual-mode spoof surface plasmon polaritons[J]. IEEE antennas and wireless propagation, 2021, 20(10)：2008-2012.

[19] LU P. InP-based THz beam steering leaky-wave antenna[J]. IEEE transactions on terahertz science and technology, 2021, 11(2)：218-230.

[20] WANG X C, ZHAO W S, HU J, et al. Reconfigurable terahertz leaky-wave antenna using graphene-based high-impedance surface[J]. IEEE transactions on nanotechnology, 2015, 14(1)：62-69.

[21] QU B, YAN S, ZHANG A, et al. Low-profile SSPP antenna with vertical polarization and omnidirectional radiation[C]//2020 IEEE MTT-S International Microwave Workshop Series on Advanced Materials and Processes for RF and THz Applications (IMWS-AMP), November 13-15, 2020, Guangzhou, China. New York：IEEE, 2020.